Two Distinct Proton Binding Sites in the ATP Synthase Family†

Christoph von Ballmoos and Peter Dimroth*

Institut für Mikrobiologie, ETH Zürich, Wolfgang-Pauli-Strasse 10, CH-8093 Zürich, Switzerland

Received June 4, 2007; Revised Manuscript Received August 20, 2007

ABSTRACT: The F_1F_0 ATP synthase utilizes energy stored in an electrochemical gradient of protons (or Na^+ ions) across the membrane to synthesize ATP from ADP and phosphate. Current models predict that the protonation/deprotonation of specific acidic c ring residues is at the core of the proton translocation mechanism by this enzyme. To probe the mode of proton binding, we measured the covalent modification of the acidic c ring residues with the inhibitor dicyclohexylcarbodiimide (DCCD) over the pH range from 5 to 11. With the H^+-translocating ATP synthase from the archaeum *Halobacterium salinarium* or the Na^+-translocating ATP synthase from *Ilyobacter tartaricus*, the pH profile of DCCD labeling followed a titration curve with a pK_a around neutral, reflecting protonation of the acidic c ring residues. However, with the ATP synthases from *Escherichia coli*, mitochondria, or chloroplasts, a clearly different, bell-shaped pH profile for DCCD labeling was observed which is not compatible with carboxylate protonation but might be explained by the coordination of a hydronium ion as proposed earlier [Boyer, P. D. (1988) *Trends Biochem. Sci. 13*, 5−7]. Upon site-directed mutagenesis of single binding site residues of the structurally resolved c ring, the sigmoidal pH profile for DCCD labeling could be converted to a more bell-shaped one, demonstrating that the different ion binding modes are based on subtle changes in the amino acid sequence of the protein. The concept of two different binding sites in the ATP synthase family is supported by the ATP hydrolysis pH profiles of the investigated enzymes.

The majority of cellular ATP is synthesized from ADP and phosphate by the ATP synthase using a transmembrane electrochemical ion gradient as an energy source. A proton motive force derived from photosynthesis or respiration drives ATP synthesis in chloroplasts, mitochondria, and most bacteria (*1*). Some anaerobic bacteria convert the energy of a decarboxylation event into an electrochemical gradient of sodium ions, which serves Na^+-translocating F_1F_0 ATP synthases as a primary driving force (*2*−*4*). Examples are the closely related enzymes from *Propionigenium modestum* and *Ilyobacter tartaricus*. The H^+- and Na^+-translocating F_1F_0 ATP synthases are phylogenetically related and share many common structural and functional features.

All ATP synthases are composed of two rotary motors, the membrane-embedded F_0 motor that translocates the coupling ions and the extrinsic F_1 motor that synthesizes the ATP. F_1 and F_0 are connected by a central and a peripheral stalk to exchange energy with each other (for a review, see ref *5*). The F_0 motor consists of a ring of c subunits which is abutted laterally by the a subunit and a dimer of b subunits. The c subunits harbor the ion binding sites that can be accessed from both sides of the membrane. There is general agreement for the location of the periplasmic entrance channel in subunit a, but the location of the exit channel is still under debate (*6*, *7*). A major difference between the H^+- and Na^+-dependent enzymes is the chemical nature of the binding sites, which shuttle the ions between the two channels. Whereas in the H^+-translocating ATP synthases a conserved acidic residue is thought to be sufficient for proton binding, at least three residues are involved in ion binding in the Na^+-translocating counterparts (*8*). The recent c oligomer and K ring structure of the Na^+-dependent enzyme of *I. tartaricus* (*9*) or *Enterococcus hirae* (*10*) showed that the Na^+ ion is liganded by four and five amino acid residues, respectively.

In the absence of Na^+, the ATP synthases of *P. modestum* and *I. tartaricus* are able to translocate protons (*11*). In the transition to this mode, the pH optimum of ATP hydrolysis is shifted from a bell-shaped profile with maximum activity between pH 7 and pH 9 to a sharp peak around pH 6.5−7 (*12*), which is thought to correspond to the pK_a of the conserved acidic c ring residues. The common H^+-translocating ATPases, however, have a broad pH profile, similar to that of the Na^+-saturated *P. modestum* enzyme. We therefore hypothesized that the different pH profiles reflect distinct proton binding sites in the ATPases.

The conserved property of the acidic residue in the c subunit from all ATP synthases to covalently react with dicyclohexylcarbodiimide (DCCD)[1] was used to investigate this paradigm (*13*). Figure 1 depicts the mechanism of this reaction as proposed by Khorana (*14*). The requirement of an exchangeable proton for the modification with DCCD implies a strong pH dependency as observed with the enzyme of *P. modestum* (*12*). In accordance with the proposed mechanism (Figure 1), the reaction velocity has its maximum in the acidic range and decreases with increasing pH with a sigmoid dependency and an inflection point around pH 7.

† This work was supported by the Swiss National Science Foundation.

* To whom correspondence should be addressed. Phone: +41 1 632 3321. Fax: +41 1 632 1378. E-mail: dimroth@micro.biol.ethz.ch.

[1] Abbreviations: DCCD, dicyclohexylcarbodiimide; MADLI-MS, matrix-assisted laser desorption ionization mass spectrometry.

10.1021/bi701083v CCC: $37.00
Published on Web 10/02/2007

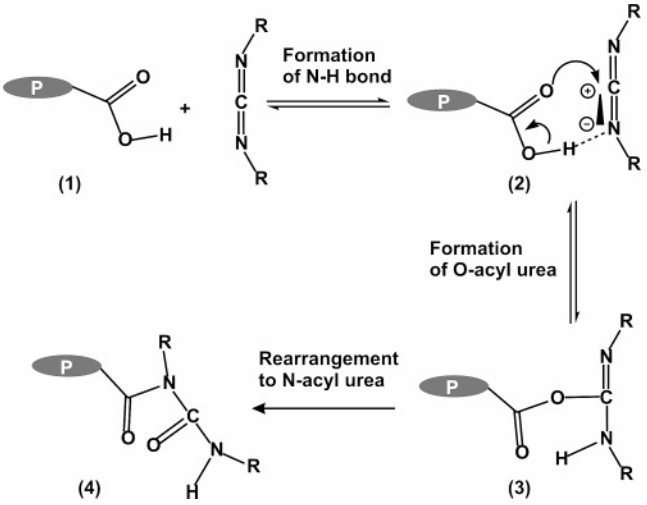

FIGURE 1: Proposed mechanism for the modification of the conserved carboxylic acid on subunit c with DCCD (*14*). In a first step, the carboxylic acid forms a hydrogen bond to one of the nitrogen atoms of the carbodiimide (**1** → **2**). Electron rearrangement leads to the formation of the unstable *O*-acylurea derivative (**2** → **3**). In the absence of a nucleophile, rearrangement of the molecule leads to the formation of the stable *N*-acylurea derivative (**3** → **4**).

Furthermore, the addition of Na^+ decreases the velocity of the modification due to the competition of Na^+ binding to the acidic residue and the concomitant displacement of the proton (*15*, *16*).

Here, we used the covalent modification of the acidic residue with DCCD to probe the proton availability at the binding site of organisms throughout the biological kingdom. For this purpose, membranes of *Halobacterium salinarium*, *I. tartaricus*, *Escherichia coli*, spinach chloroplasts, and bovine mitochondria were incubated with DCCD at varying pH values, and the modification of the acidic residues was monitored by MALDI mass spectrometry.

MATERIALS AND METHODS

Bacterial Growth and Tissue Origin. *E. coli atp* deletion strain DK8 was transformed with plasmid pBWU13 carrying the *atp* operon, except for *atpI* (*17*). Cells were grown in LB medium, harvested in the late exponential phase, and stored at −80 °C. *I. tartaricus* cells were grown under anaerobic conditions as described (*18*). Spinach (*Spinacia oleracea*) leaves were obtained from the local market. Bovine heart was obtained from the local slaughterhouse and was kept at 4 °C for 16 h between slaughter and homogenization. Cultured cells from the strain *H. salinarium* SNOB were a gift from J. Tittor from the Max-Planck-Institute of Biochemistry in Martinsried, Germany. Strain *H. salinarium* R9 (no gas vacuoles) was a gift from H. Strahl and K. H. Altendorf from the University of Osnabrück, Germany, and was cultured as described (*19*).

Preparative Procedures. The preparation of *E. coli* membranes and their solubilization with cholate/deoxycholate in the presence of 1 M KCl was performed as described (*20*, *21*). Membranes from *I. tartaricus* cells were prepared and solubilized with Triton X-100 as described (*18*).

A total of 1.5−2 kg of spinach leaves was used to prepare thylakoid membranes as described (*22*). The ATP synthase was solubilized from the membranes and fractionated by ammonium sulfate precipitation and subsequent sucrose density gradient centrifugation as described (*22*).

A total of 0.9−1 kg of bovine heart was used to prepare mitochondria as described (*23*). The protein content of the collected mitochondria was adjusted to 20 mg/mL, and the preparation was stored at −20 °C. Solubilization of bovine mitochondria with dodecyl maltoside was performed as described (*24*).

Cells collected from a culture of *H. salinarium* were washed twice in 50 mM Tris−HCl, pH 8, 4 M NaCl and ruptured by osmotic shock with deionized water. The mixture was stirred to homogeneity, and the membranes were collected by ultracentrifugation (200000*g*, 4 °C, 60 min) and washed twice with the buffer indicated. Alternatively, cells were resuspended in the buffer described above and were broken in a French press apparatus (2×18000 psi, 1.2×10^8). Cell debris was removed by centrifugation (10000*g* at 4 °C, 10 min), and the membranes were collected by ultracentrifugation (200000*g*, 4 °C, 60 min) and washed twice with the buffer indicated.

ATP Hydrolysis Activity Measurements. Membranes of *E. coli* and *P. modestum* were prepared as described and suspended in 10 mM Tris−HCl, pH 8, 2.5 mM $MgCl_2$ (10−15 mg of protein/mL). F_1 from *E. coli* ATP synthase was prepared by stripping the membrane fraction with 1 mM Tricine−HCl, pH 8.5, 0.2 mM EDTA, 10% glycerol. After ultracentrifugation (200000*g*, 4 °C, 45 min), the supernatant was collected and used as the F_1 fraction. ATP hydrolysis measurements were performed using the coupled assay as described (*25*). Assay buffer was prepared as described (*25*), but only weakly buffered with 5 mM potassium phosphate, pH 7−8, with special care to check and adjust the pH of the buffer after preparation to avoid precipitation of enzymes. The assay buffer (AB) was split into buffer AB1 and AB2. The latter was supplemented with 50 mM buffer (final concentration) of the desired pH value and 2 mM ATP. For the pH range from 5 to 9, 50 mM MMT (50 mM MES, 50 mM MOPS, 50 mM tricine, adjusted to the desired pH with 5 M KOH) was used, whereas for more alkaline pH, tricine was replaced by 2-(*N*-cyclohexylamino)ethanesulfonic acid (CHES). Membrane samples or the F_1 fraction was mixed with buffer AB1, containing 1 μM 2-*n*-heptyl-4-hydroxyquinoline *N*-oxide (HQNO) to minimize free NADH oxidation in native membranes, and aliquots of 100 μL were pipetted into the wells of a 96-well quartz plate. The reaction was then started with the addition of 150 μL of buffer AB2, and the OD_{340} was monitored in a 96-well plate reader (BioRad) and used to calculate ATP hydrolysis rates as described (*25*). In parallel, measurements without the addition of ATP were performed to obtain the free NADH oxidation rates in membranes (<10%). To guarantee coupling of ATP hydrolysis and ion transport, ATP hydrolysis activities of membranes preincubated with 100 μM DCCD for 2 h at 4 °C were measured. Good coupling (>85%) was observed in the relevant pH range from 5 to 9.5. After the reaction, pH values were measured directly in the reaction vessel. Triplicates of every data point were collected, and two individual measurements were performed.

Determination of Na^+ Activation on ATP Hydrolysis Activity. The coupled enzyme assay was prepared as described (*25*) with the following modifications. To minimize the Na^+ content of the assay mixture, the potassium salt of

NADH was used, and the hydrolysis reaction was initiated by the addition of Tris−ATP. The residual Na^+ concentration was below 50 μM as determined with atomic absorption spectroscopy (Shimadzu AA-6200). The reaction was monitored at 340 nm in a UVIKON 940 spectrophotometer. Na^+ was added stepwise from a 5 M NaCl solution, and the activities were taken after equilibration. Shown are the average values of three measurements.

Preparation and Purification of Recombinant I. tartaricus ATP Synthase. The *unc* operon of *I. tartaricus* was amplified from genomic DNA and cloned into the expression vector pTrc99A. Expression of this plasmid results in the production of a functional Na^+-dependent ATP synthase (unpublished data). Mutations cSer66Ala and cTyr70Phe were introduced using PCR-based cloning techniques. Plasmids harboring wild-type and mutant ATP synthases were transformed in *E. coli* DK8, lacking the *atp* operon, and cultured in LB medium, and expression was induced with 1 mM IPTG at $OD_{600} = 0.7$. Enrichment of ATP synthases by fractionated PEG precipitation was performed as described (*21*).

Modification of c Subunits with DCCD. To prevent continued DCCD modification of ATP synthase c subunits after organic extraction, as observed by Hermolin and Fillingame (*26*), we included an additional step in our protocol. Prior to the addition of organic solvents, 1 M ammonium acetate buffer, pH 7, was mixed with the samples to balance their different pH values to ~7. This ensures similar extraction conditions for all samples. Furthermore, we reasoned that an excess of acetic acid (from ammonium acetate) would act as a scavenger of free DCCD molecules, which remain in solution after organic extraction. It was not necessary to concentrate the organic phase for mass spectrometry. In general, we spotted a small aliquot of the samples right after extraction on the matrix-coated target plate for the mass spectrometry instrument. In control experiments, we spotted a small aliquot of the extracted sample (stored at −80 °C) a few hours and several weeks after the extraction. Under the conditions described and used, we did not observe a continued labeling of c subunits. Moreover, no more than one DCCD molecule bound per molecule c subunit was observed. All incubations were performed at room temperature.

Method A. A 50 μL sample of membrane preparation (10−15 mg/mL) or the detergent-extracted enzyme (2−4 mg/mL) was diluted into 450 μL of incubation buffer. For the pH range from 5 to 9, MMT (100 mM MES, 100 mM MOPS, 100 mM tricine, 5 mM $MgCl_2$, adjusted to the desired pH with 5 M KOH) was used, whereas, for more alkaline pH values, tricine was replaced by CHES. DCCD was added at the desired concentration using stock solutions prepared in ethanol with the volume of ethanol added ≤1% of the total reaction volume. At the desired time points, samples of 30 μL were taken and mixed with 20 μL of 1 M ammonium acetate to adjust the pH to near 7. The samples were immediately mixed with 500 μL of chloroform/methanol (1:1) and shaken vigorously. The subsequent addition of 100 μL of H_2O induced a phase separation, which was completed by centrifugation (10000*g*, room temperature, 1 min). The c subunit-containing samples in the organic solvent were stored at −80 °C prior to MALDI measurements.

Method B. Method A was optimized for use in the 96-well format. All pipetting reactions were performed with multichannel pipets or a multidispense pipet to guarantee reproducibility. A 3 μL sample of membrane preparation (10−15 mg/mL) or purified enzyme (2−4 mg/mL) was diluted with 17 μL of buffer at the desired pH value (buffer composition; see method A) and placed into a 0.2 mL 96-well PCR plate (polypropylene). The reaction was started by the addition of 1 μL of a DCCD stock solution in 20% ethanol, and the plate was mildly shaken during the course of the reaction. At the desired time points, aliquots of 10 μL from the reaction mixture were transferred to a new 96-well plate and mixed with 100 μL of chloroform/methanol/1 M ammonium acetate (10:10:1). Phase separation was induced by the addition of 20 μL of distilled water, completed by centrifugation of the plate (3000*g*, room temperature, 5 min), and the lower organic phase was transferred into a new 96-well plate and directly used for mass spectrometry.

MADLI-TOF Measurements. Molecular masses were determined on a 4700 proteomics analyzer from Applied Biosystems, a MALDI-TOF instrument equipped with a reflector. Different matrixes were tested, but if not otherwise stated, a 10 mg/mL solution of dihydroxybenzoic acid (DHB) in acetonitrile:H_2O (0.1% TFA) = 2:1 was used. An amount of 0.7 μL of matrix was placed onto the target plate and allowed to dry before 0.2−0.5 μL of the chloroform phase of the DCCD-modified sample was applied to the matrix-coated spot. Measurements were performed in the linear mode to minimize sample decomposition as observed previously (*27*).

RESULTS

MALDI-TOF as a Quantitative Tool for Analysis of Subunit c Labeling by DCCD. It has been well documented that DCCD inhibits the ATP synthase by specifically modifying the conserved acidic residues of subunit c, which are thought to comprise (part of) the binding sites of the coupling ions. In previous studies, this reaction has been followed by the inhibition of ATP hydrolysis activity. Since a single DCCD-modified c subunit is sufficient to block ATP hydrolysis completely (*26*), only the kinetics of the first DCCD binding event per molecule has been observed in these experiments (see below).

In the assay described below, we utilized the unique property of subunit c to become highly enriched from any kind of sample by a chloroform/methanol extraction and subsequent phase separation induced by water (*28*). A small aliquot of the subunit c-containing organic phase can directly be applied to MALDI mass spectrometry (*27*). To quantify the amount of labeling, we used an internal standard in the form of the unmodified c subunit. Subunit c labeling can therefore be related to the ratio of labeled to unlabeled c subunit in individual measurements (Supporting Information Figure 1).

pH Dependence of Subunit c Labeling from Different ATP Synthases by DCCD. In a first series of experiments, the method described above was applied to measure DCCD labeling kinetics of the *I. tartaricus* ATP synthase at different pH values. For this purpose, isolated *I. tartaricus* membranes (Figure 2a), the detergent solubilized ATP synthase, or the purified enzyme (data not shown) were incubated with DCCD at the pH values indicated. The modification of subunit c was stopped by rapid mixing with an excess of

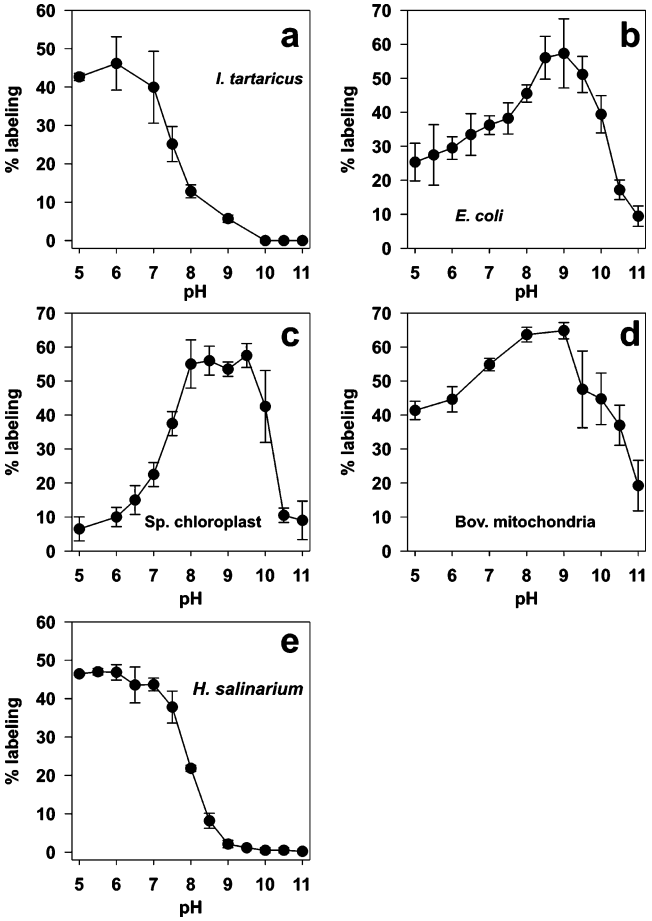

FIGURE 2: pH dependence for the modification of c subunit binding sites of various ATP synthases by DCCD using method A. **(a)** Membranes of *I. tartaricus* cells were prepared and incubated with 100 μM DCCD at different pH values (5 min) as described in the Materials and Methods. Peak intensities from labeled (L) and unlabeled (U) c subunits were used to determine the ratio L/(U + L), which was plotted against the pH values indicated. Depicted are the mean values and the standard deviations (error bars) of at least three measurements. **(b)** Like (a), but with isolated membranes of *E. coli* cells (15 min). **(c)** Like (a), but with sucrose density gradient purified F_1F_0 ATP synthase from spinach chloroplasts (15 min). **(d)** Like (a), but with isolated mitochondria from bovine heart (10 min). **(e)** Like (a), but with isolated membranes of *H. salinarium* (20 min).

chloroform/methanol followed by phase separation upon addition of water. An aliquot of the lower organic phase was then spotted onto a layer of dried matrix on the target plate for mass spectrometry. The results from all three sample preparations were very similar and showed the expected sigmoidal pH dependency of the modification (Figure 2a). The profiles were also similar to those obtained by previous DCCD labeling experiments, and these were not distinct between the *I. tartaricus* ATP synthase or its isolated c ring (*16*), which indicates no interference of other subunits with the DCCD labeling of subunit c under these conditions.

For the purposes of this study it was important to determine the protonation status of the c subunit binding sites outside the influence of subunit a. This meant that the measurements performed were based on the labeling of a significant number of c subunits. To account for different labeling rates, the incubation times with DCCD were adjusted to obtain ~50% of the maximum labeling levels (all c subunits modified). Hence, the representations in Figure 2 do not reflect accurate initial reaction rates, but rather a comparison of reaction velocities at different pH values. Control experiments, however, showed that the pH differences in subunit c labeling are more pronounced under our conditions and the observed effects are therefore not artificially broadened by rate saturation.

The pH profile for the modification of subunit c from *E. coli* membranes is shown in Figure 2b. Measurements with detergent-solubilized membranes produced essentially the same results (data not shown). The profile is entirely different from that found with the *I. tartaricus* ATP synthase, showing an increase in the labeling velocity between pH 5.5 and pH 9.0 and a strong decrease between pH 9.5 and pH 11. First, these data show that the acidic residue is not completely shielded from the pH of the medium, as has been suggested (*29*). Second, the significant decrease of the modification rate at lower pH is unexpected and is not congruent with a mechanism that requires the protonation of the acidic amino acid prior to its modification. As a proton is, however, mandatory for the chemical modification of the acidic c ring residue by DCCD (see the introduction), an attractive hypothesis is that these enzymes use hydronium ion binding rather than group protonation as the mechanism of proton binding. It is not entirely clear why the chemical labeling reaction slows at the acidic pH values, where the carboxylates are expected to become protonated. Possibly, the hydronium ion acts as a better proton donor than the protonated carboxylate in this artificial chemical reaction.

This unexpected finding prompted us to extend our studies to H^+-translocating enzymes from other organisms. The results obtained with the isolated chloroplast ATP synthase are depicted in Figure 2c. The pH profile of DCCD labeling is rather similar to that of the *E. coli* enzyme, except for an even more pronounced decrease in the labeling rate in the acidic pH range. In contrast to the *E. coli* enzyme, the chloroplast ATP synthase reacts poorly at pH 5 and the labeling rate reaches its maximum velocity at pH 8, followed by a plateau, and a sharp decrease toward more alkaline pH values.

We further tested the ATP synthase from bovine heart mitochondria (Figure 2d). With either whole mitochondria or detergent-extracted protein, similar pH profiles for the DCCD labeling were obtained. The pH profile closely resembles the one found for the *E. coli* enzyme, showing significant labeling at pH 5 and a small increase in the labeling rate on increasing the pH to 8−9. The rate of DCCD labeling decreases again if the pH is raised further into the more alkaline pH range.

Finally, with membranes of *H. salinarium*, a halophilic archaeum, a pH profile completely different from those of the other H^+-translocating ATPases was found that closely resembled the one from the *I. tartaricus* ATP synthase in the H^+-translocating mode (in the absence of Na^+ ions). The data in Figure 2e show the highest rates of subunit c labeling at pH 5−6 and decreasing labeling rates at higher pH values following a titration curve with a pK_a around 7.5 which probably corresponds to the membrane-buried carboxylic acid of the ATP synthase.

Mutational Analysis of the Binding Site in the I. tartaricus c Ring. The recent crystal structure of the c ring of *I. tartaricus* revealed two new aspects concerning the ion binding site. First, the backbone carbonyl of Val63 makes a

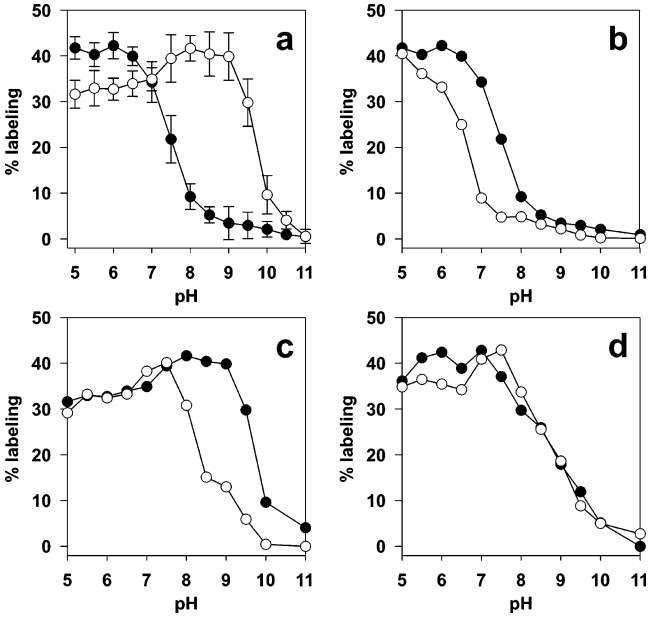

FIGURE 3: pH profiles for DCCD modification of binding site mutants in the *I. tartaricus* ATP synthase. The same procedure as described in Figure 2 was followed with the exception that recombinantly expressed ATP synthase was modified with DCCD using method B. Depicted are the mean values and the standard deviations (error bars) of at least three independent measurements. **(**a**)** pH profiles of the wild type (●) and the cTyr70Phe mutant (○). **(**b**)** pH profiles of the wild-type enzyme in the absence (●) and the presence (○) of 15 mM Na^+. **(**c**)** pH profiles of the cTyr70Phe mutant enzyme in the absence (●) and the presence (○) of 15 mM Na^+. **(**d**)** pH profiles of the cSer66Ala mutant enzyme in the absence (●) and the presence (○) of 15 mM Na^+. For clarity, error bars were omitted in (b)−(d).

direct contact with the Na^+ ion. This allows the helix to kink below Val63, and the ring becomes hourglass shaped. Second, Tyr70 makes a contact with Glu65, orienting its phenol group toward the binding site. However, it becomes clear from the structure that a complex hydrogen bond network stabilizes the binding pocket and the coordination of Na^+ is the result of a finely tuned scaffold within the three involved helices. In this site, Glu65 not only delivers its negative charge to the Na^+ ion, but also acts as the key point of the scaffold, providing hydrogen bonding with Gln32, Ser66, and Tyr70 simultaneously. We therefore rationalized that the replacement of Tyr70 by phenylalanine might have an impact on the scaffold and on Na^+ binding, without being directly involved in Na^+ coordination. For this purpose, the mutants Tyr70Phe and Ser66Ala were created. The latter serves as a control for a Na^+-impaired binding site as demonstrated with the closely related enzyme of *P. modestum* (*8*). The results of Figure 3 show the pH profiles for subunit c labeling of recombinant wild-type and mutant *I. tartaricus* ATP synthases. The recombinantly expressed wild-type enzyme showed the typical sigmoidally shaped profile, which was shifted to more acidic pH values by Na^+ addition. A similar profile, but with a shift to more alkaline pH values, was obtained for the Ser66Ala mutant. These data indicate that the pK_a of Glu65 increased from about 7.5 in the wild type to about 8.5 in the mutant ATP synthase, probably reflecting the replacement of the polar serine by the more hydrophobic alanine. As might be expected from the impairment of the Na^+ binding site, the addition of 15 mM Na^+ had no effect on the pH labeling profile of the

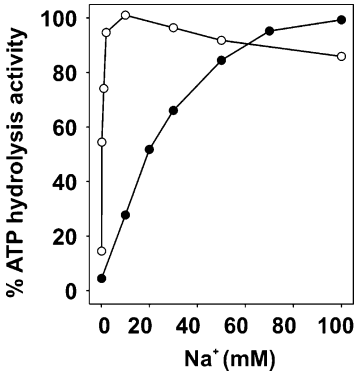

FIGURE 4: Activation by Na^+ of ATP hydrolysis activity of the purified ATP synthase from *I. tartaricus*. Recombinantly expressed ATP synthase of either the wild type (○) or the Y70F mutant (●) was used to determine the activation of ATP hydrolysis activity by Na^+ ions, using the coupled enzyme assay. Na^+-poor chemicals were used throughout the experiment. The initial Na^+ concentration was below 80 μM, as verified by atomic absorption spectroscopy. Increasing amounts of NaCl were added to the solution, and the activities were determined by following the decrease in absorption at 340 nm. Shown are the average values of three measurements.

ATP synthase with Ser66Ala mutation. Strikingly, the shape of the pH profile of the Tyr70Phe mutant drastically changed from the sigmoidal form to the more bell-shaped profile of the proton-dependent enzymes. In the presence of 15 mM Na^+, similar labeling rates were observed between pH 5 and pH 8, and at higher pH values the labeling rate decreased more rapidly than in the Na^+-free controls, where high labeling rates extended up to pH 9. These results indicate that the Tyr70Phe mutant retains the ability to bind Na^+, albeit with significantly lower affinity than the wild-type enzyme. Indeed, for half-maximal ATPase activity of the mutant enzyme, about 20 mM Na^+ is required (Figure 4), whereas the wild-type enzyme exhibits half-maximal ATPase activity at ~0.5 mM Na^+ under the same conditions (*18*). Hence, disturbing the hydrogen-bonding scaffold around Glu65 by the Tyr70Phe mutation severely affects the binding of Na^+ to the binding sites on the c ring.

Taken together, these results indicate different modes of proton binding within the ATP synthase family and interconversion of one mode to the other by subtle changes of the ion binding site residues.

ATP Hydrolysis Profiles. It has been well documented that the ATP hydrolysis activity of the coupled Na^+-translocating enzyme of *P. modestum* depends on the occupation of the ion binding sites with the appropriate coupling ion (Na^+, Li^+, H^+) (*11*, *15*). We therefore rationalized that following the ATP hydrolysis of various ATP synthases dependent on the coupling ion concentration (Na^+ or H^+) might be another means to monitor occupancy of their ion binding sites.

Figure 5 shows the pH profiles for the ATP hydrolysis activities of the ATP synthases from *P. modestum*, *E. coli*, and *H. salinarium*. Under Na^+-saturated, physiological conditions, the Na^+-dependent ATP synthase from *P. modestum* shows a bell-shaped pH profile with a broad optimum ranging from pH 7 to pH 9. The pH profile is similar to that of the separated F_1 portion, showing that rate-limiting steps in F_0 are not involved under saturating Na^+ concentrations. At lower Na^+ concentrations, however, the ATPase activities of the holoenzyme decreased to reach undetectable levels without Na^+ addition at pH 8 or above. Under these

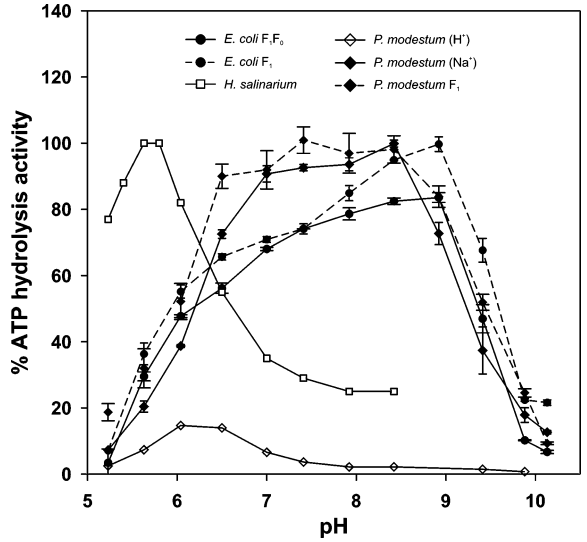

FIGURE 5: pH profiles of ATP hydrolysis activities from ATP synthases of different organisms. For clarity, the rates are scaled to reach 100% for the maximal observed activity for each organism. Maximal rates for each organism are reported below. Shown are the profiles of the purified enzyme of *P. modestum* (F_1F_0) in the presence (◆) or absence (◇) of saturating Na^+ concentrations and its separated F_1 part (◆, ---) (10 U/mg of protein). Further depicted are the profiles of the holoenzyme (●, ---) and the F_1 part (●, —) of the *E. coli* ATP synthase from native membranes (13 U/mg of protein) and the purified ATP synthase of *H. salinarium* (0.24 U/mg of protein) (□, taken from ref *46*).

conditions, therefore, delivery of Na^+ to the F_0 binding sites becomes rate limiting. In the absence of Na^+, the enzyme resumes to hydrolyze ATP with concomitant H^+ pumping by increasing the proton concentration to pH 6−7 (*11*), indicating that the H^+-ATPase activity of this enzyme strongly depends on this elevated proton concentration. Compared to that of the Na^+-saturated ATPase or the F_1 part alone, the H^+-activated activity is drastically reduced, obviously reflecting suboptimal functioning with the non-physiological coupling ion. A pH profile with a peak at pH 6.0 and significantly decreasing activities at pH > 6.5−7 is also observed for the H^+-translocating ATPase of *H. salinarium*, which therefore seems to use a proton binding mode similar to that of the *P. modestum* enzyme. Curiously, the pH profile of the *E. coli* ATPase is significantly distinct from that of the *H. salinarium* enzyme or the *P. modestum* enzyme in its H^+-translocation mode, but similar to that of the enzyme in its Na^+-translocating mode. Hence, slightly suboptimal activities are observed at pH values around 7, reported to be the pK_a of the cAsp61 residues in a chloroform/methanol water mixture (*30*), and instead, a broad pH optimum extends from pH 7.5 to pH 9. This feature is similar to the pH profile of the DCCD labeling reaction (see above) and thus in accordance with the occupation of the binding sites over a broad pH range. The pH dependence of the ATPase activity of F_1 from *E. coli* was very similar to that of the coupled F_1F_0 complex, indicating that the protonation of the binding sites is not the rate-limiting step in the ATP-driven rotation of the holoenzyme. A similar broad pH profile for the coupled ATP hydrolysis activity is also reported for the enzymes of bovine mitochondria and spinach chloroplast (*31*, *32*). In analogy to the Na^+-dependent enzymes, the low occupancy of cAsp61 with protons well above its pK_a should become rate limiting, however, if the group protonation mechanism is valid. We therefore hypothesize that the coupled *E. coli* ATPase does not rely on the protonation of cAsp61, but rather on a different mode of proton binding in its immediate vicinity.

DISCUSSION

The rotational mechanism of ATP synthesis depends on the flux of the coupling ions across the membrane down their chemical and/or electrical gradients. Whereas the known Na^+-translocating ATP synthases are mostly restricted to certain anaerobic bacteria, their H^+-translocating counterparts are widely distributed throughout the biological kingdom. Crucial for ion transport and coupled rotation are the specific ion binding sites on the c ring. Loading and unloading of these sites at defined positions of the rotating c ring shuttles the ions between the input and output channels. Insight into the architecture and chemical properties of the ion binding sites was obtained from the recent crystal structures of the c or K ring from the Na^+-dependent F-ATP synthase of *I. tartaricus* and the V-ATPase of *E. hirae*, respectively (*9*, *10*). In the *I. tartaricus* c ring, the Na^+ ions are coordinated by four oxygen atoms within a scaffold that is defined by multiple hydrogen bonds (Figure 6a). The carboxyl group of the conserved acidic residue (cGlu65) not only contributes one of its oxygens as a Na^+-binding ligand, but also acts as a recipient of hydrogen bonds from Gln32, Ser66, and Tyr70. This hydrogen-bonding network stabilizes the conformation of the Na^+ binding site between the three different helices involved.

In a simple model of the F_0 motor, the universally conserved stator arginine 210 in *E. coli* is positioned between two binding sites of the c ring (*33*, *34*). One of these is in contact with the input, and the other one is in contact with the output channel of the ion (Figure 6b). These designations refer to one direction of rotation and become the opposite if the rotation is reversed. The suggested role of the positively charged arginine is to facilitate the dissociation of the ion from the approaching rotor site into the appropriate release channel (*35*). Implicit in the model is the recharging of the empty binding site that has passed the stator arginine from the appropriately located input channel. The channels are thought to be aqueous in accordance with accessibility studies with hydrophilic probes (*6*, *7*), and therefore, recharging the site will be most efficient if the environmental ion concentration exceeds the binding site's dissociation constant for the ion. This hypothesis is in good agreement with a dissociation constant for Na^+ from the binding site of ∼0.5 mM and a K_m for Na^+ of ∼1 mM in activating the ATP hydrolysis activity of the *P. modestum* enzyme (*12*).

To test the group protonation model experimentally, we monitored the proton availability at the binding sites by the modification of subunit c by DCCD. For the Na^+-dependent ATP synthase of *P. modestum*, the rate of DCCD labeling follows a titration curve with a pK_a of ∼7, representing the degree of protonation of the acidic residue. A remarkably similar sigmoidal pH profile was found for the modification of the ATP synthase from the archaeum *H. salinarium*, which suggests a group protonation mechanism for this physiological H^+-translocating enzyme as well.

For all other H^+-translocating ATP synthases tested (covering enzymes from eubacteria, chloroplasts, and mito-

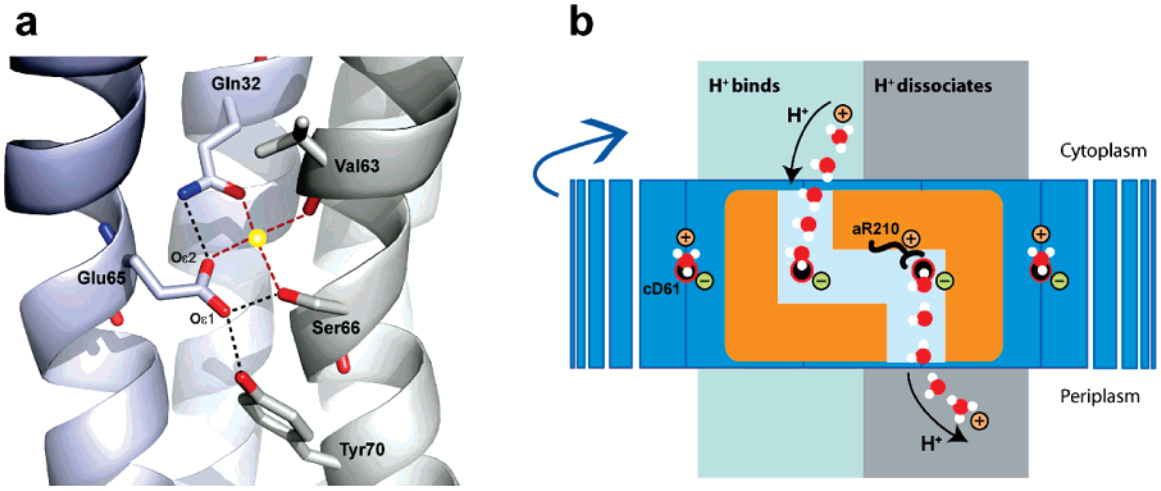

FIGURE 6: (a) Close-up of the Na^+ ion binding site in the c ring of the *I. tartaricus* ATP synthase (modified from ref *9*). The Na^+ ion is coordinated by the side chain oxygens of residues Glu65 and Gln32 on one c subunit and residue Ser66 and the backbone carbonyl of Val63 on the neighboring subunit. Oxygens Oϵ1 and Oϵ2 from Glu65 accept hydrogen bonds from Ser66 and Tyr70 and from Gln32, respectively. **(**b**)** Model for proton translocation involving hydronium ion coordination in the *E. coli* ATP synthase. Depicted are the rotor c ring (blue) and the stator a subunit (orange). Their common interface harbors the critical residues during torque generation and ion translocation. During ATP hydrolysis, the c ring rotates counterclockwise and protons enter the a/c interface from the cytoplasm and are pumped across the membrane into the periplasmic reservoir. An occupied binding site enters the a/c interface from the right and reaches the water-filled outlet channel in subunit a. The conserved stator arginine lowers both the affinity of the hydronium ion and the pK_a of the cAsp61. This forces the proton to leave the coordinated hydronium ion and be transmitted along a water wire into the periplasmic reservoir. After passing the stator arginine the hydronium ion binding site is allowed to re-form and can accept a proton from the cytoplasm through the water-filled inlet channel in subunit a (or within the a/c interface). The reoccupied binding site can now exit the a/c interface, and the next cycle is allowed to take place. Thereby, the high-affinity hydronium ion binding site allows the enzyme to efficiently bind and translocate protons over a broad pH range.

chondria), however, partial bell-shaped pH profiles with a broad optimum in the alkaline pH range (around 8−9) for DCCD labeling are observed, not obeying the rule for protonation of a carboxylic residue. The inconsistency with a group protonation mechanism is particularly evident from the decreasing DCCD labeling rates at lower pH values, most strikingly observed with the enzyme of spinach chloroplasts. This corroborates with an earlier finding that ATP hydrolysis in spinach chloroplasts was almost unaffected by DCCD at pH 5, whereas the enzyme was completely inhibited at pH 8 under the same conditions (*36*). In these enzymes, therefore, not the protonated carboxylate but a different functional group has to act as the proton donor of the modification reaction (Figure 1). It cannot be completely ruled out that factors other than the proton availability influence the reaction rate of DCCD with subunit c of the ATP synthase, e.g., a conformational change within the c ring, altering the accessibility of the binding site to the surface. In the structure of the *I. tartaricus* c ring, which was crystallized at pH 4.5, however, no such conformational change or exposure of the reactive carboxylic side chain was observed. In the case of the chloroplast enzyme, which works predominantly at low pH (pH 5 in the lumen), no large structural changes within subunit c can be expected. In general, we believe that the membrane acts as a conserving shell for the amino acids that are not in direct contact with the aqueous phase, and therefore, major influences from the outside pH on the conformation are not expected. Because of the very hydrophobic nature of DCCD, the molecule is expected to enter the membrane rapidly and therefore should not influence the reaction rate under different conditions.

It is interesting that pH profiles similar to those observed for the DCCD modification reaction are also found for ATP hydrolysis activities. In the *H. salinarium* ATP synthase and the H^+-coupled *P. modestum* ATP synthase, this activity has its optimum at pH ≈ 6.5 and rapidly decreases to undetectable levels at pH 8 and above. In the H^+-translocating ATP synthases of *E. coli*, mitochondria, or chloroplasts, however, the pH optimum is much broader and clearly shifted into the alkaline range. Interestingly, the ATP hydrolysis profile of F_1 of *P. modestum*, a representative of the first group of enzymes, is also broad and indistinguishable from that of Na^+-saturated F_1F_0. These results seem to indicate that the ATP hydrolysis activity in F_1F_0 is determined by the properties of F_1 under conditions where the F_0 binding sites are saturated with the appropriate coupling ion as in Na^+-saturated F_1F_0. However, when the F_0 sites are only partially occupied or empty as in the H^+- or Na^+-coupled *P. modestum* enzyme at pH > 7 or at nonsaturating Na^+ concentrations, respectively, the F_0 part becomes rate limiting for ATP hydrolysis activity.

These interpretations are corroborated by a comparison of the ATP hydrolysis activities of F_1 and F_1F_0 of *E. coli*, a representative of the second class of enzymes. These activities are practically identical over the entire pH range from 6 to 10, thus indicating that the activity of the F_1F_0 holoenzyme is not limited by a suboptimal occupancy of the F_0 binding sites. Hence, the H^+ occupancy of the first class of enzymes, which is limited to the acidic to neutral pH range, as shown by the DCCD labeling experiments, is reflected by the narrow ATP hydrolysis profile of the F_1F_0 holoenzyme around pH 6−7. In contrast, the H^+ site occupancy over a broad range, as observed by DCCD labeling in the second class of enzymes, is reflected by the broad ATP hydrolysis pH profile of the corresponding F_1F_0 holoenzyme.

The potential of the second class of ATP synthases to bind protons over a broad pH range may also be important for

the proton translocation mechanism. It has been suggested that protonation and deprotonation of the F_0 sites is facilitated by different pK_a values of the conserved acidic residues during contact to either side of the membrane. Implicit in this model is a pK_a exceeding that of the environmental proton concentration during protonation and a pK_a below the environmental proton concentration during proton release. It is commonly accepted that the conserved stator charge arginine aids in proton release by decreasing the dielectric permittivity of the membrane, which lowers the pK_a of the acidic residue. One cannot rationalize, however, an increase of the pK_a of the acidic residue in the interface with subunit a over that in the interface with lipids. Nevertheless, a broad pH profile of $\Delta\psi$-driven proton transport is observed with F_0 of spinach chloroplasts and *Rhodobacter capsulatus* (*34*, *37*). To account for these data, the membrane potential was assumed to influence the pK_a of the acidic binding site residues on either side of the membrane (for details, see ref *34*). Our experiments, however, were performed in solution or in nonenergized membranes and thus in the absence of a membrane potential, yet indicated broad pH profiles for DCCD labeling or ATP hydrolysis activities. These data therefore suggest that protons can be bound to the F_0 sites in the absence of a membrane potential even at high environmental pH values. Therefore, the idea of alternative ion coordination (see below) is an additional piece of information toward the understanding of proton transport in F_0 motors. With the model described above, it would have been difficult to explain the broad pH range during ATP hydrolysis, since no external driving force can accommodate the pK_a required to load the site at the high pH values in solution.

In 1988, Boyer hypothesized that proton and Na^+ ion coordination would be much more related if the H^+ were coordinated together with a water molecule to form H_3O^+. He pointed out that both hydronium ions and Na^+ ions can be coordinated by crown ethers. The phenomenon of related H^+ and Na^+ binding is also visible by the Na^+/H^+ exchanger monensin as revealed from its crystal structure (*38*). In the free acid form, the carboxyl group is used not only to bind the proton, but also to circularize the molecule to a crown ether-like structure with a bound water molecule in the cavity. This conformation allows a defined hydrogen-bonding scaffold, on which the positive charge of the proton is distributed. Upon Na^+ binding, the water is displaced, and the Na^+ becomes coordinated by several oxygens.

The idea of an alternative proton binding site was also postulated for H^+-translocating P-type ATPases of plants (*39*) and the lactose permease from *E. coli* (*40*) and experimentally shown for the light-driven H^+ pump bacteriorhodopsin (*41*, *42*).

A hydronium ion, coordinated by the unprotonated carboxylate and additional ligands, might also be a candidate for the majority of H^+-translocating ATP synthases. It is clear that the binding of a hydronium ion at pH 7.5−9 requires a high-affinity binding site. With such a site the operation range of the enzyme would not be restricted to pH values around the pK_a of the conserved acidic c ring residues, but could be extended widely into the alkaline pH range. It is obvious that such a high-affinity hydronium ion binding site must not be present in the Na^+-translocating ATP synthases with their 5 orders of magnitude lower Na^+ binding affinities, and indeed, these enzymes rely on a group protonation mechanism in their proton translocation mode. An efficient means to prevent the binding of a hydronium ion is to donate protein intrinsic hydrogen bonds to the oxygen atoms of the acidic c ring residues, as observed in the structure of the Na^+ binding site of the *I. tartaricus* ATP synthase (Figure 6a). With the two hydrogen bonds donated from Ser66 and Tyr70 to Oϵ1 and another hydrogen bond donated from Gln32 to Oϵ2 of Glu65 only the latter oxygen can accept one hydrogen bond from a hydronium ion, whereas with no or only one hydrogen bond donated to either of these oxygens hydronium ion binding could be stabilized by two hydrogen bonds. Taking these considerations into account, it is intriguing that, in all Na^+-translocating ATP synthases, the three amino acids of the hydrogen-bonding network (Gln32, Ser66, and Tyr70) are conserved and that no proton-translocating ATP synthase is known to date which has both Ser66 and Tyr70 residues. Further evidence along these lines stems from a comparison of the pH profile for DCCD labeling of the *I. tartaricus* wild-type and cTyr70Phe mutant enzymes. The sigmoidal pH profile of the wild type is dramatically shifted to a more bell-shaped form with a maximum in the alkaline pH range in the mutant which lacks one of the Oϵ1 hydrogen bonds and might therefore be able to coordinate a hydronium ion. The alkaline shift is also observed in the cSer66A mutation, but is somewhat less pronounced than in the Tyr70Phe mutation, which might be explained by subtle differences in the hydronium ion binding constants. These mutations affect not only the mode of proton binding but also that of Na^+ binding, leading to a severely reduced affinity in the Tyr70Phe mutant or its complete extinction in the Ser66A mutant. A similar situation might be present in the enzyme of *H. salinarium*, which is also dependent on group protonation. Sequence comparison of the two c subunits shows additional hydrophilic residues (Tyr, Glu, and Arg on the inner helix, Pro and Thr on the outer helix) in the close proximity of the conserved acidic residue, which might impair hydronium ion binding by a hydrogen-bonding scaffold similar to that observed in the *I. tartaricus* enzyme (Supporting Information Figure 2). In the H^+-dependent enzymes, hydrophilic residues around the binding site are significantly less abundant.

In spite of the different ion binding modes of the ATP synthases, these enzymes are closely related in using ion translocation across the membrane to induce intersubunit rotation. It is not surprising, therefore, that the c subunits share many structural elements such as the helical hairpin organization and the acidic residue in the middle of the membrane providing ion binding.

Such a strong relationship raises the idea of a common evolutionary precursor. Since sequence elements and functionality of the protonation-dependent binding mechanism are still found in Na^+-dependent enzymes, one might speculate that the mechanism in the archaeum *H. salinarium* is the most ancient form of coupling ion binding in ATP synthases, whereas Na^+ and H_3O^+ binding enzymes have evolved to adapt to different environments. In this context, it is interesting to note that the corresponding enzymes of a few other archaebacteria were also shown to have an acidic pH optimum for ATP hydrolysis. They are therefore good candidates for similar protonation-dependent enzymes (*43*−*45*).

ACKNOWLEDGMENT

We thank Peter Gehrig for advice during the MALDI-TOF measurements, and Fabienne Henzen, Carole Bürgi Taboada Merino, and Judith Zingg-Ebneter for excellent technical assistance. We thank Gregory Cook for critical reading of the manuscript. MALDI-TOF measurements were performed at the Functional Genomics Center Zürich (FGCZ).

SUPPORTING INFORMATION AVAILABLE

MALDI mass spectra (Figure S1), a c subunit sequence alignment (Figure S2) as mentioned in the text, and sigmoidal fittings to the profiles (Figure S3). This material is available free of charge via the Internet at http://pubs.acs.org.

REFERENCES

1. Boyer, P. D. (1997) The ATP synthase- a splendid molecular machine, *Annu. Rev. Biochem. 66*, 717−749.
2. Laubinger, W., and Dimroth, P. (1987) Characterization of the Na^+-stimulated ATPase of *Propionigenium modestum* as an enzyme of the F_1F_0 type, *Eur. J. Biochem. 168*, 475−480.
3. Dimroth, P., von Ballmoos, C., Meier, T., and Kaim, G. (2003) Electrical power fuels rotary ATP synthase, *Structure (London) 11*, 1469−1473.
4. Dimroth, P., von Ballmoos, C., and Meier, T. (2006) Catalytic and mechanical cycles in F-ATP synthases. Fourth in the Cycles Review Series, *EMBO Rep. 7*, 276−282.
5. Capaldi, R. A., and Aggeler, R. (2002) Mechanism of the F_1F_0-type ATP synthase, a biological rotary motor, *Trends Biochem. Sci. 27*, 154−160.
6. Angevine, C. M., and Fillingame, R. H. (2003) Aqueous access channels in subunit a of rotary ATP synthase, *J. Biol. Chem. 278*, 6066−6074.
7. Angevine, C. M., Herold, K. A., and Fillingame, R. H. (2003) Aqueous access pathways in subunit a of rotary ATP synthase extend to both sides of the membrane, *Proc. Natl. Acad. Sci. U.S.A. 100*, 13179−13183.
8. Kaim, G., Wehrle, F., Gerike, U., and Dimroth, P. (1997) Molecular basis for the coupling ion selectivity of F_1F_0 ATP synthases: probing the liganding groups for Na^+ and Li^+ in the c subunit of the ATP synthase from *Propionigenium modestum*, *Biochemistry 36*, 9185−9194.
9. Meier, T., Polzer, P., Diederichs, K., Welte, W., and Dimroth, P. (2005) Structure of the rotor ring of F-Type Na^+-ATPase from *Ilyobacter tartaricus*, *Science 308*, 659−662.
10. Murata, T., Yamato, I., Kakinuma, Y., Leslie, A. G., and Walker, J. E. (2005) Structure of the rotor of the V-Type Na^+-ATPase from *Enterococcus hirae*, *Science 308*, 654−659.
11. Laubinger, W., and Dimroth, P. (1989) The sodium ion translocating adenosinetriphosphatase of *Propionigenium modestum* pumps protons at low sodium ion concentrations, *Biochemistry 28*, 7194−7198.
12. Kluge, C., and Dimroth, P. (1993) Kinetics of inactivation of the F_1F_0 ATPase of *Propionigenium modestum* by dicyclohexylcarbodiimide in relationship to H^+ and Na^+ concentration: probing the binding site for the coupling ions, *Biochemistry 32*, 10378−10386.
13. Graf, T., and Sebald, W. (1978) The dicyclohexylcarbodiimide-binding protein of the mitochondrial ATPase complex from beef heart. Isolation and amino acid composition, *FEBS Lett. 94*, 218−222.
14. Khorana, H. G. (1953) The Chemistry of Carbodiimides, *Chem. Rev. 53*, 145−166.
15. Kluge, C., and Dimroth, P. (1993) Specific protection by Na^+ or Li^+ of the F_1F_0-ATPase of *Propionigenium modestum* from the reaction with dicyclohexylcarbodiimide, *J. Biol. Chem. 268*, 14557−14560.
16. Meier, T., Matthey, U., von Ballmoos, C., Vonck, J., Krug von Nidda, T., Kühlbrandt, W., and Dimroth, P. (2003) Evidence for structural integrity in the undecameric c-rings isolated from sodium ATP synthases, *J. Mol. Biol. 325*, 389−397.
17. Moriyama, Y., Iwamoto, A., Hanada, H., Maeda, M., and Futai, M. (1991) One-step purification of Escherichia coli H(+)-ATPase (F0F1) and its reconstitution into liposomes with neurotransmitter transporters, *J. Biol. Chem. 266*, 22141−22146.
18. Neumann, S., Matthey, U., Kaim, G., and Dimroth, P. (1998) Purification and properties of the F_1F_0 ATPase of *Ilyobacter tartaricus*, a sodium ion pump, *J. Bacteriol. 180*, 3312−3316.
19. Oesterhelt, D., and Stoeckenius, W. (1974) Isolation of the cell membrane of *Halobacterium halobium* and its fractionation into red and purple membrane, *Methods Enzymol. 31*, 667−678.
20. Fillingame, R. H., and Foster, D. L. (1986) Purification of F_1F_0 H(+)-ATPase from *Escherichia coli*, *Methods Enzymol. 126*, 545−557.
21. von Ballmoos, C., Meier, T., and Dimroth, P. (2002) Membrane embedded location of Na^+ or H^+ binding sites on the rotor ring of F_1F_0 ATP synthases, *Eur. J. Biochem. 269*, 5581−5589.
22. Turina, P., Samoray, D., and Gräber, P. (2003) H^+/ATP ratio of proton transport-coupled ATP synthesis and hydrolysis catalysed by CF_0F_1-liposomes, *EMBO J. 22*, 418−426.
23. Smith, A. L. (1967) Preparation, Properties, and Conditions for Assay of Mitochondria: Slaughterhouse Material, Small-scale, *Methods Enzymol. 10*, 81−86.
24. Buchanan, S. K., and Walker, J. E. (1996) Large-scale chromatographic purification of F_1F_0-ATPase and complex I from bovine heart mitochondria, *Biochem. J. 318*, 343−349.
25. Laubinger, W., and Dimroth, P. (1988) Characterization of the ATP synthase of *Propionigenium modestum* as a primary sodium pump, *Biochemistry 27*, 7531−7537.
26. Hermolin, J., and Fillingame, R. H. (1989) H^+-ATPase activity of *Escherichia coli* F_1F_0 is blocked after reaction of dicyclohexylcarbodiimide with a single proteolipid (subunit c) of the F_0 complex, *J. Biol. Chem. 264*, 3896−3903.
27. von Ballmoos, C., Appoldt, Y., Brunner, J., Granier, T., Vasella, A., and Dimroth, P. (2002) Membrane topography of the coupling ion binding site in Na^+-translocating F_1F_0 ATP synthase, *J. Biol. Chem. 277*, 3504−3510.
28. Fillingame, R. H. (1975) Identification of the dicyclohexylcarbodiimide-reactive protein component of the adenosine 5′-triphosphate energy-transducing system of *Escherichia coli*, *J. Bacteriol. 124*, 870−883.
29. Valiyaveetil, F., Hermolin, J., and Fillingame, R. H. (2002) pH dependent inactivation of solubilized F_1F_0 ATP synthase by dicyclohexylcarbodiimide: pK(a) of detergent unmasked aspartyl-61 in *Escherichia coli* subunit c, *Biochim. Biophys. Acta 1553*, 296−301.
30. Assadi Porter, F. M., and Fillingame, R. H. (1995) Proton-translocating carboxyl of subunit c of F_1F_0 H^+-ATP synthase: the unique environment suggested by the pKa determined by 1H NMR, *Biochemistry 34*, 16186−16193.
31. Dorgan, L. J., and Schuster, S. M. (1981) The effect of nitration and D2O on the kinetics of beef heart mitochondrial adenosine triphosphatase, *J. Biol. Chem. 256*, 3910−3916.
32. Takabe, T., and Hammes, G. G. (1981) pH dependence of adenosine 5′-triphosphate synthesis and hydrolysis catalyzed by reconstituted chloroplast coupling factor, *Biochemistry 20*, 6859−6864.
33. Elston, T., Wang, H., and Oster, G. (1998) Energy transduction in ATP synthase, *Nature 391*, 510−513.
34. Feniouk, B. A., Kozlova, M. A., Knorre, D. A., Cherepanov, D. A., Mulkidjanian, A. Y., and Junge, W. (2004) The proton-driven rotor of ATP synthase: ohmic conductance (10 fS), and absence of voltage gating, *Biophys. J. 86*, 4094−4109.
35. Wehrle, F., Kaim, G., and Dimroth, P. (2002) Molecular mechanism of the ATP synthase's F_0 motor probed by mutational analyses of subunit a, *J. Mol. Biol. 322*, 369−381.
36. Mills, J. D., and Hind, G. (1979) Light-induced Mg^{2+} ATPase activity of coupling factor in intact chloroplasts, *Biochim. Biophys. Acta 547*, 455−462.
37. Althoff, G., Lill, H., and Junge, W. (1989) Proton channel of the chloroplast ATP synthase, CF0: Its time-averaged single-channel conductance as function of pH, temperature, isotopic and ionic medium composition, *J. Membr. Biol. 108*, 263−271.
38. Lutz, W. K., Winkler, F. K., and Dunitz, J. D. (1971) Crystal structure of the antibiotic monensin similarities and differences betweeen free acid and metal complex, *Helv. Chim. Acta 54*, 1103−1108.
39. Fraysse, A. S., Moller, A. L., Poulsen, L. R., Wollenweber, B., Buch-Pedersen, M. J., and Palmgren, M. G. (2005) A systematic mutagenesis study of Ile-282 in transmembrane segment M4 of the plasma membrane H^+-ATPase, *J. Biol. Chem. 280*, 21785−21790.

40. Johnson, J. L., Lockheart, M. S., and Brooker, R. J. (2001) A triple mutant, K319N/H322Q/E325Q, of the lactose permease cotransports H^+ with thiodigalactoside, *J. Membr. Biol. 181*, 215−224.
41. Garczarek, F., Brown, L. S., Lanyi, J. K., and Gerwert, K. (2005) Proton binding within a membrane protein by a protonated water cluster, *Proc. Natl. Acad. Sci. U.S.A. 102*, 3633−3638.
42. Garczarek, F., and Gerwert, K. (2006) Functional waters in intraprotein proton transfer monitored by FTIR difference spectroscopy, *Nature 439*, 109−112.
43. Inatomi, K. (1986) Characterization and purification of the membrane-bound ATPase of the archaebacterium *Methanosarcina barkeri*, *J. Bacteriol. 167*, 837−841.
44. Lubben, M., and Schafer, G. (1987) A plasma-membrane associated ATPase from the thermoacidophilic archaebacterium, *Sulfolobus acidocaldarius*, *Eur. J. Biochem. 164*, 533−540.
45. Wakagi, T., and Oshima, T. (1985) Membrane-bound ATPase of a thermoacidophilic archaebacterium, *Sulfolobus acidocaldarius*, *Biochim. Biophys. Acta 817*, 33−41.
46. Mukohata, Y., and Yoshida, M. (1987) The H^+-translocating ATP synthase in *Halobacterium halobium* differs from F_0F_1-ATPase/synthase, *J. Biochem. (Tokyo) 102*, 797−802.

BI701083V